Eur. Phys. J. B **17**, 261–268 (2000)

THE EUROPEAN PHYSICAL JOURNAL B

EDP Sciences

Analysis of brittle coating fragmentation under uniaxial tension for Weibull strength distributions

J. Andersons[a], U.A. Handge, I.M. Sokolov, and A. Blumen

Theoretical Polymer Physics, University of Freiburg, Hermann-Herder-Str. 3, 79104 Freiburg i.Br., Germany

Received 16 February 2000

Abstract. We investigate the sequential cracking of thin brittle coatings attached adhesively to substrates. The focus of our study are uniaxial tensile loading conditions, where we monitor the behavior in a continuous picture and the coating strength follows a two-parameter Weibull distribution. For fracture well under way we derive an approximate analytical expression for the distribution of fragment lengths. We recover that the distribution scales with the average fragment length $\langle l \rangle$ and that $\langle l \rangle$ is a power function of the applied strain ε, *i.e.* $\langle l \rangle \propto \varepsilon^{-\kappa}$, where κ depends on the distribution of the strength of the coating and on the adhesive's nonlinearity. Furthermore we compare our approximate analytical expression with numerical solutions and with simulations' findings.

PACS. 05.40.-a Fluctuation phenomena, random processes, noise, and Brownian motion – 46.65.+g Random phenomena and media – 46.50.+a Fracture mechanics, fatigue and cracks

1 Introduction

Disorder aspects play a central role in failure phenomena (which determine the strength properties of solids) and render very complex the prediction of the resistance of solids to stress. Thus, calculations of materials' strength based only on interatomic potentials lead to values which are typically orders of magnitude larger than what is observed [1]. This is due both to the probabilistic extreme-value character of crack initiation and also to the multi-scale nature of the phenomena accompanying crack propagation. Crack nucleation and propagation are namely determined by the microstructure of the materials under investigation [2] and depend strongly on the samples' past history. On the other hand, breakage which arises as a consequence of sequential processes, say in coatings under tensile load [3–5] and in surface layers which desiccate [6–9], leads to qualitatively similar patterns for vastly different materials. This is a clear indication of the existence of universality in fragmentation, which suggests that the parameters which govern sequential cracking are of restricted number. The analysis of previous research relates these parameters to the disorder of the failure probabilities in the coating [10–14] and to the law (linear or nonlinear [15,16]) which determines the stress transfer between coating and support.

Several research groups have addressed in this decade the problem of the interplay between disorder and elasticity by using discrete models [12,17–19]; these are particularly suited to follow the sequential process of pattern formation in a quasi-microscopic way. On the other hand, engineering mechanics descriptions use continuous probabilistic pictures [20–24]. Here we will stress the connection between the two approaches, focusing mainly on the Weibull distribution of probabilities of failure, which is related to one of the three possible stable asymptotic laws for the distribution of extrema [25]. In so doing, we will determine approximate solutions for the fragment length distribution of the ensuing fracture patterns and will recover the scaling of the mean fragment length as a function of the applied strain, while extending previous results.

We now turn to the microscopic parameters governing fragmentation and focus on uniaxial stress. Under such stress the problem often simplifies, as shown by numerical results [26] and by experiments [3–5]: one has then a practically one-dimensional picture, in which series of quasi-parallel cracks form perpendicular to the direction of the stress. The condition under which such patterns obtain depend on the length scales involved in the problem. Thus in previous works [11,12,18,22] a correlation length ξ was introduced, which is a measure of the load transfer efficiency; it is defined as being that distance from the border of a fragment at which the stress recovers a value close to that which prevails well-inside a very large fragment. The important role played by ξ was emphasized in reference [22], where the special case of perfect plasticity is discussed. Thus the relation between ξ and other characteristic length scales of the system allows to distinguish between different fragmentation regimes. Moreover, ξ determines whether fragmentation under uniaxial load proceeds in an effectively one-dimensional manner or whether the process is truly two-dimensional. The first case is realized in situations with weak disorder and also

[a] *Permanent address:* Institute of Polymer Mechanics, University of Latvia, Aizkraukles 23, Riga LV 1006, Latvia

when the coating has the form of a narrow strip of width W, such that $W < \xi$. For strong disorder and/or large W the development of cracks after nucleation depends very much on the material at hand: both strong disorder (scatter along the crack's path) and the proximity of other growing cracks let the problem retain its two-dimensional character. We concentrate in what follows only on effectively 1-d situations and discuss analytical and numerical approaches for determining the probability distributions of fragment lengths.

This article is organized as follows: In Section 2 we derive the stress distribution in a short fragment. In Section 3 we discuss the failure probability in a fragment and its connection to Weibull strength distributions. In Section 4 we display the kinetic equation and derive approximate solutions for several distinct cases. Section 5 is devoted to the comparison of our analytical and numerical solutions to the results obtained from simulations. The paper closes with conclusions in Section 6.

2 Stress distribution in a small fragment

Several models in the physical literature on failure phenomena start from mesoscopic lattice models [2], based on networks consisting of springs [27]. The springs representing the coating are assumed to be breakable, their equilibrium length being $l_{\rm eq}$. The nodes of the coating are attached to the substrate *via* elastic (possibly nonlinear) bonds (*i.e.* leaf springs). Now, as shown in reference [18], the one-dimensional variant of this model is amenable to an analytical solution. Reference [15] was devoted to the investigation of the case in which the bonds between the coating and the substrate behave nonlinearly. In the continuum limit the equations which describe the stress distribution go over into those of the shear-lag model, introduced much earlier by Cox [28]. In what follows, we discuss the situation in more detail and display (starting from a continuous picture) the pertinent equations.

Consider thus a fragment of length l and of thickness $h_{\rm c}$ attached to a substrate *via* a (nonlinearly) elastic adhesive layer of thickness $h_{\rm a}$. The substrate is subjected to a uniaxial tensile loading, characterized by the applied strain ε. For a thin planar coating the only component of the stress of interest here is the one parallel to the load. Then the condition that forces are in equilibrium reads $\mathrm{d}\sigma/\mathrm{d}y = \tau/h_{\rm c}$, where the y axis is parallel to the load, $\sigma(y)$ is the stress in the coating, and $\tau(y)$ is the shear stress in the adhesive.

Similarly to the analysis of fragmentation in references [4,15] we assume that the adhesive is nonlinearly elastic and approximate the shear stress-strain relation through:

$$\tau = C\mathrm{sgn}(\gamma)|\gamma|^m \tag{1}$$

with positive parameters C and m. The shear strain γ is given by $\gamma = (u_{\rm c} - u_{\rm s})/h_{\rm a}$, where $u_{\rm c}$ and $u_{\rm s}$ denote the displacement of the coating and of the substrate, respectively. For a linearly elastic adhesive $m = 1$ holds, and the factor C coincides with the shear modulus. In the case of $m < 1$, equation (1) provides a rough approximation of strain-hardening plasticity response upon active loading [29]. For $m = 0$ we deal with perfect plasticity, *cf.* reference [22]. On the other hand, $m > 1$ describes the increase of the modulus with strain, as often occurs in elastomers.

For a linearly elastic coating $\sigma = E_{\rm c}\mathrm{d}u_{\rm c}/\mathrm{d}y$ holds, where $E_{\rm c}$ is the Young's modulus of the coating. Inserting $\sigma = E_{\rm c}\mathrm{d}u_{\rm c}/\mathrm{d}y$ into the balance equation $\mathrm{d}\sigma/\mathrm{d}y = \tau/h_{\rm c}$, one obtains the following nonlinear second order differential equation for $u_{\rm c}(y)$:

$$\frac{\mathrm{d}^2 u_{\rm c}}{\mathrm{d}y^2} = \mathrm{sgn}(\gamma)\frac{C}{E_{\rm c}h_{\rm c}h_{\rm a}^m}|u_{\rm c} - u_{\rm s}|^m. \tag{2}$$

If the effect of coating cracks on the deformation of the substrate is negligible, then the strain everywhere in the substrate is equal to the applied strain ε, and consequently $u_{\rm s}$ is easily determined. Due to the symmetry of the problem, it suffices to consider only half of the fragment. Taking the origin of the y axis in the fragment center, one has $u_{\rm s} = \varepsilon y$, and we obtain for $y \geq 0$

$$\frac{\mathrm{d}^2 u_{\rm c}}{\mathrm{d}y^2} = -\frac{C}{E_{\rm c}h_{\rm c}h_{\rm a}^m}(\varepsilon y - u_{\rm c})^m. \tag{3}$$

The boundary conditions are $u_{\rm c}(0) = 0$ and $u_{\rm c}'(l/2) = 0$.

For a fragment short with respect to the length of the zone of stress transfer, $l \ll \xi$, the displacement of the substrate exceeds by far that of the coating, *i.e.* $\varepsilon y \gg u_{\rm c}$. Neglecting $u_{\rm c}$ on the rhs of equation (3), we obtain the following stress distribution in the fragment:

$$\sigma(y) = \frac{C\varepsilon^m l^{m+1}}{2^{m+1}(m+1)h_{\rm c}h_{\rm a}^m}\left(1 - \left|\frac{2y}{l}\right|^{m+1}\right). \tag{4}$$

An analogous expression for the strain in the coating has been found in the analysis of networks made out of springs [15].

For the subsequent analysis, it is convenient to represent the stress distribution in the form $\sigma = w_0(\varepsilon)f(x,l)$, with $x \in [0,l]$. Setting $w_0(\varepsilon) = C\varepsilon^m/[2^{m+1}(m+1)h_{\rm c}h_{\rm a}^m]$ and $y = x - l/2$ leads to

$$f(x,l) = l^{m+1}\left(1 - \left|\frac{2x}{l} - 1\right|^{m+1}\right). \tag{5}$$

The shape of the stress distribution along the fragment is given by the function $f(x,l)$, which depends strongly on the adhesive's deformability, characterized by the parameter m. Figure 1 shows $f(x,l)$ for $l = 1$ and several m values. For $m = 0$ the function $f(x,l)$ increases linearly from the fragment's edges, while for $m = 1$ it is a parabola. With increasing m the plateau in the middle of the fragment gets more and more pronounced.

3 Probability of fragment failure

Coatings have defects, such as micropores and flaws, which occur during the manufacturing process and which are

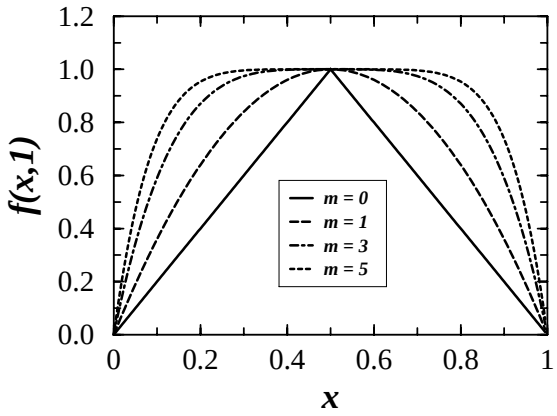

Fig. 1. The function $f(x,1)$, see equation (5), plotted for $m = 0, 1, 3$ and 5; $f(x,1)$ is proportional to the stress in a fragment. For $m = 0$ the function $f(x,1)$ consists of two straight parts, for $m = 1$ it is a parabola. With increasing m the plateau in the middle of the fragment gets more pronounced.

randomly distributed. Consequently, the strength of a coating element is statistically distributed as well. In this section we consider the failure of a layer under increasing stress and assume that the coating's strength follows a two-parameter Weibull distribution. According to this distribution, the probability of failure $P(\Delta x, \sigma)$ of a coating element of length Δx at stress σ is given by:

$$P(\Delta x, \sigma) = 1 - \exp\left[-\Delta x \left(\frac{\sigma}{\omega}\right)^{\alpha}\right], \tag{6}$$

where α and ω are the shape and the scale parameters.

The Weibull distribution [30] of continuum mechanics, widely applied in the engineering literature for the description of the materials' strength, corresponds in a lattice model picture to a power function distribution for the local breakdown thresholds, as used in references [15,18]. To recall this we consider an element of length Δx, being part of a fragment which is small enough to allow to view the forces and the displacements on it to be constant, but large enough to contain a large number of breakable subunits of length a, *i.e.* $N = \Delta x/a \gg 1$. The element will break when its first weakest subunit will break. In the spring model of reference [18] a special case of the cumulative probability distribution function of the local breakdown strength $\sigma_{\rm b}$ has the form

$$P(\sigma_{\rm b}) = \left(\frac{\sigma_{\rm b}}{\omega}\right)^{\alpha} \tag{7}$$

for $0 \le \sigma_{\rm b} \le \omega$ and $P(\sigma_{\rm b}) = 0$ otherwise. In the notation of equation (37) of reference [18] (MSB) $i_{\min} = 0$, $\alpha = \alpha_{\rm MSB} + 1$ and $\omega = W_{\rm MSB}$. Hence the local breakdown strength is bounded. Assuming this form of the spring model also here leads for the failure probability $P_N(\sigma)$ of the fragment to $P_N(\sigma) = 1 - [1 - P(\sigma)]^N = 1 - \exp[N \ln(1 - P(\sigma))]$. For $N \gg 1$ the typical breakdown value σ is small and the corresponding probability distribution tends to the asymptotic form $P_N(\sigma) = 1 - \exp[-N(\sigma/\omega)^{\alpha}] = 1 - \exp[-\Delta x \sigma^{\alpha}/(a\omega^{\alpha})]$, *i.e.* to the Weibull form. Thus equation (7) used in the spring model leads in the continuum to the Weibull-form, equation (6). We note here that the Weibull distribution is one of the three possible stable asymptotic laws for the distribution of extrema, namely the one which is always attained when the values of $\sigma_{\rm b}$ are bounded [25].

The form of $P(\Delta x, \sigma)$, equation (6), is very advantageous and allows for a simpler analytical approach to fragmentation than was possible in the general case of equation (37) of reference [18], case considered in references [12,18]. For a stress distribution in the form $\sigma(x) = w_0(\varepsilon) f(x,l)$, it is convenient to define the loading parameter s so that $s = (w_0(\varepsilon)/\omega)^{\alpha}$. Moreover we introduce the coating stress parameter $t = s f^{\alpha}(x,l)$. Then the probability that a coating element of length Δx fails at t^* having survived t is

$$P(\Delta x, t^*|t) = 1 - \exp\left[-(t^* - t)\Delta x\right]. \tag{8}$$

The probability $P_-(l, s^*|s)$ that a fragment of length l fails under the load s^*, having survived s, is related to the probability that each of the coating elements survives by:

$$\begin{aligned} P_-(l, s^*|s) &= 1 - \prod_i \left[1 - P\left(\Delta x_i, t_i^*|t_i\right)\right] \\ &= 1 - \exp\left[-\sum_i (t_i^* - t_i)\Delta x_i\right] \end{aligned} \tag{9}$$

which reads in the continuum limit:

$$P_-(l, s^*|s) = 1 - \exp\left[-(s^* - s)\int_0^l f^{\alpha}(x,l)\,{\rm d}x\right]. \tag{10}$$

Hence the probability density $p_-(l,s)$ for a fragment of length l to fail under a load increment ${\rm d}s$, while having survived s, is given by:

$$p_-(l,s) = \left.\frac{\partial P_-(l, s^*|s)}{\partial s^*}\right|_{s^*=s} = \int_0^l f^{\alpha}(x,l)\,{\rm d}x. \tag{11}$$

Now consider the probability $P_+(x, t^*|t)$ of a failure in the interval x to $x + \Delta x$, again under the load s^* having survived s. This probability equals to the probability that the coating element in question fails times the probability that there are no failures in the rest of the fragment:

$$\begin{aligned} P_+(x, t^*|t) = &\left(1 - \exp\left[-(t^* - t)\Delta x\right]\right) \\ &\times \exp\left[-\int_0^x (t^* - t)\,{\rm d}x - \int_{x+\Delta x}^l (t^* - t)\,{\rm d}x\right]. \end{aligned} \tag{12}$$

For very small Δx, one can expand the first exponential term on the rhs of equation (12). This yields

$$\begin{aligned} P_+(x, s^*|s) = &\,{\rm d}x(s^* - s) f^{\alpha}(x,l) \\ &\times \exp\left[-(s^* - s)\int_0^l f^{\alpha}(x,l)\,{\rm d}x\right]. \end{aligned} \tag{13}$$

Therefore the probability density $p_+(x,l,s)$ for a fragment of length l to fail between x and $x+\mathrm{d}x$ upon a load increment $\mathrm{d}s$ having survived s is:

$$p_+(x,l,s)\,\mathrm{d}x = \left.\frac{\partial P_+(x,s^*|s)}{\partial s^*}\right|_{s^*=s} = f^\alpha(x,l)\,\mathrm{d}x. \quad (14)$$

Since $p_-(l,s)$ is the density of the probability for the whole fragment to fail and $p_+(x,l,s)$ denotes the density of the probability to fail at some point x, the function $p_-(l,s)$ follows from $p_+(x,l,s)$ by integration: $p_-(l,s) = \int_0^l p_+(x,l,s)\,\mathrm{d}x$.

It should be noted that the obtained probability densities equations (11) and (14) are strictly exact only under particular loading conditions, namely if a fragment of a given length undergoes without failure a monotonic increase of the load from 0 to s^*. This condition is strictly met only for the very first fragment, since the other fragments are themselves the result of previous fragmentations and therefore have a much richer, in general, non-monotonic loading history, which is not accounted for in equations (11) and (14). This might somewhat overestimate the failure probabilities, especially for fragment elements located close to fragment edges.

4 Fragmentation equation and its solutions

With increasing applied strain ε the number of fragments of a given length changes, since fragments can break and new fragments are created. The fragmentation kinetics is determined by the balance between fragment generation and breakup. As is customary in fragmentation phenomena [21,31–33] and in related physical situations such as the creation of contacts in light fibrous materials [34] one considers an equation for the global process. In this study we assume that the following fragmentation equation for the number density of fragments $n(l,s)$ holds:

$$\frac{\partial n(l,s)}{\partial s} = -p_-(l,s)n(l,s) + 2\int_l^\infty p_+(l,x,s)n(x,s)\,\mathrm{d}x. \quad (15)$$

The change $\partial n/\partial s$ of the function $n(l,s)$ results from the breakup and the generation of fragments. The first term on the rhs of equation (15) considers that fragments of length l break with a certain probability. The second term takes into account that fragments whose fragment length x is larger than l can break at the position l or $x-l$. The factor 2 in equation (15) results from the fact that the probability to fail at the position l equals the probability to fail at the position $x-l$. Note that in the integral on the rhs of equation (15) l and x have been changed in comparison with equation (14). In equation (15) we assume implicitly that breakage events create only two new pieces out of an old one. Inserting equations (5, 11, 14) into equation (15) yields:

$$\frac{\partial n(l,s)}{\partial s} = -n(l,s)l^{\alpha(m+1)+1}\int_0^1 \left(1-|1-2t|^{m+1}\right)^\alpha \mathrm{d}t + 2\int_l^\infty n(x,s)x^{\alpha(m+1)}\left(1-|1-2l/x|^{m+1}\right)^\alpha \mathrm{d}x. \quad (16)$$

Obviously, due to the kernel of the integral, equation (16) is not easy to handle. In this article, we make use of two methods to determine approximate solutions to this integro-differential equation. First, we derive analytical expressions based on a rough approximation of the kernel. Second, we solve numerically the kinetic equation for the special case $m=1$ and α integer. In both cases we concentrate on the advanced stages of fragmentation, where the initial condition $n(l,0)=\delta(l-N)$ for an intact coating of length N does not influence the fragment length distribution anymore.

4.1 Approximate analytical solution

A rough simplification of the kinetic equation (16) can be achieved by neglecting the contribution of fragments of length around l to the generation of fragments of length l. We then expand the term in brackets of the second summand on the rhs of equation (16) for $x \gg 2l$ and retain the first-order term only, *i.e.* $1-|1-2l/x|^{m+1} \approx 2(m+1)l/x$. Inserting this expression into equation (16) leads to

$$\frac{\partial n(l,s)}{\partial s} = -n(l,s)Al^{\alpha(m+1)+1} + Bl^\alpha\int_l^\infty n(x,s)x^{\alpha m}\,\mathrm{d}x, \quad (17)$$

where we introduced the constants $A = \int_0^1 \left(1-|1-2t|^{m+1}\right)^\alpha \mathrm{d}t$ and $B = 2^{\alpha+1}(m+1)^\alpha$. As can be readily verified by insertion, the solution of equation (17) is:

$$n(l,s) = s^c l^\alpha \exp\left(-Asl^\lambda\right) \quad (18)$$

with $\lambda = \alpha(m+1)+1$ and $c = B/(A\lambda)$. From this we obtain the average fragment length $\langle l\rangle$:

$$\langle l\rangle = \frac{\int_0^\infty l\,n(l,s)\,\mathrm{d}l}{\int_0^\infty n(l,s)\,\mathrm{d}l} = \frac{\Gamma[(\alpha+2)/\lambda]}{\Gamma\left[(\alpha+1)/\lambda\right]}(As)^{-1/\lambda}, \quad (19)$$

where $\Gamma(x)$ denotes the Gamma function. Inserting $s = (w_0(\varepsilon)/\omega)^\alpha$ into equation (19), we find that the mean fragment length scales with the applied strain ε as $\langle l\rangle \propto \varepsilon^{-\alpha m/[\alpha(m+1)+1]}$, which result has been also derived in the context of spring-networks, see reference [15]. As also discussed in this article, the scaling of $\langle l\rangle$ with ε is well supported by simulations. In order to obtain the fragment length distribution density $\rho(l,s)$, we have to normalize the solution equation (18). Hence we have

$$\rho(l,s) = \frac{n(l,s)}{\int_0^\infty n(l,s)\,\mathrm{d}l} = \frac{\lambda l^\alpha (As)^{(\alpha+1)/\lambda}}{\Gamma[(\alpha+1)/\lambda]}\exp\left(-Asl^\lambda\right). \quad (20)$$

Numerical investigations [18] have shown that in the later stages the fragment length distribution keeps its shape when plotted as a function of $\zeta = l/\langle l\rangle$, *i.e.* it fulfills the relation $\rho(l,s) = \langle l\rangle^{-1} p(\zeta)$, where $p(\zeta)$ does not depend on s. This behaviour indicates that fragmentation proceeds universally. Thus experimental results, when plotted as a function of ζ, should be depicted by $p(\zeta)$, on which we now focus. The distribution function equation (20) also fulfills the relation $\rho(l,s) = \langle l\rangle^{-1} p(\zeta)$ with

$$p(\zeta) = k_1 k_2^{\alpha+1} \zeta^{\alpha} \exp\left[-(k_2\zeta)^{\lambda}\right], \tag{21}$$

where we set $\zeta = l/\langle l\rangle$. The constants k_1 and k_2 only depend on the Weibull shape parameter α and the nonlinearity parameter m, and are given by $k_1 = \lambda/\Gamma[(\alpha+1)/\lambda]$ and $k_2 = \Gamma[(\alpha+2)/\lambda]/\Gamma[(\alpha+1)/\lambda]$.

We close the section by considering the limiting case $m \to \infty$. For m very large the probability density $p_+(x,l,s)$ ceases to depend on the position x of the failure, as follows from equations (5) and (14). Hence $p_+(x,l,s)$ is approximately given by

$$p_+(x,l,s)\,\mathrm{d}x = \frac{\mathrm{d}x}{l} \int_0^l f^{\alpha}(\tilde{x},l)\,\mathrm{d}\tilde{x}. \tag{22}$$

Then the fragmentation equation (15) reads

$$\frac{\partial n(l,s)}{\partial s} = -n(l,s) A l^{\lambda} + 2A \int_l^{\infty} n(x,s) x^{\lambda-1}\,\mathrm{d}x. \tag{23}$$

The solution of equation (23) is $n(l,s) = s^{2/\lambda} \exp\left(-A s l^{\lambda}\right)$, which implies for the average fragment length:

$$\langle l\rangle = \frac{\Gamma(2/\lambda)}{\Gamma(1/\lambda)} (As)^{-1/\lambda}. \tag{24}$$

Consequently, the fragment length distribution $p(\zeta)$ with $\zeta = l/\langle l\rangle$ is given by

$$p(\zeta) = k_3 k_4 \exp\left[-(k_4\zeta)^{\lambda}\right], \tag{25}$$

where the constants k_3 and k_4 are defined by $k_3 = \lambda/\Gamma(1/\lambda)$ and $k_4 = \Gamma(2/\lambda)/\Gamma(1/\lambda)$. For m very large equation (25) simplifies to

$$p(\zeta) = \frac{\lambda \exp\left[-(\zeta/2)^{\lambda}\right]}{2\Gamma(1/\lambda)}\,. \tag{26}$$

In the limit $m \to \infty$ equation (26) leads to $p(\zeta) = \theta(2-\zeta)/2$, where $\theta(x)$ denotes the Heaviside function. For $m \to \infty$ the peak of the distribution $p(\zeta)$ disappears. This is due to the fact that in the limit $m \to \infty$ the shape of the stress distribution attains a large plateau. Hence cracks can occur at any position within the fragment with the same probability.

4.2 Numerical integration

In this section we present a numerical solution for the rate equation (16) in the special case $m = 1$ (linear stress transfer) and for integer α values. The studies of references [5,12,15,18] and the previous section have shown that in advanced stages of fragmentation the average fragment length scales with the applied strain. In fact the whole fragment length *distribution* $\rho(l,s)$ obeys a universal form, see references [12,18] and also equation (21) here, since $p(\zeta) = \langle l\rangle \rho(l,s)$ with $\zeta = l/\langle l\rangle$ holds. These observations suggest another approach for solving the kinetic equation (16). Knowing that $n(l,s)$ attains in advanced fragmentation stages the form $p(\zeta) = \langle l\rangle\rho(l,s)$, we look for a solution of equation (16) using the scaling Ansatz $n(l,s) = s^{c_1}\varphi(s^{c_2}l)$, where $\varphi(z)$ is a function of $z = s^{c_2}l$ only. One may note that the previously obtained approximate solution, equation (18), also has this scaling form, with $c_1 = (B/A - \alpha)/\lambda$, $c_2 = 1/\lambda$ and $\varphi(z) = z^{\alpha}\exp(-Az^{\lambda})$. The Ansatz $n(l,s) = s^{c_1}\varphi(s^{c_2}l)$ allows now to derive an ordinary differential equation from equation (16). In line with related studies of rate equations [31,32,34] we look for an asymptotic solution.

Introducing the variable $z = s^{c_2}l$, we find $\partial n/\partial s = c_1 s^{c_1-1}\varphi(z) + c_2 s^{c_1+c_2-1} l\varphi'(z)$, where the prime denotes differentiation with respect to z. We first consider the case $m = 1$ and $\alpha = 1$. Inserting $n(l,s) = s^{c_1}\varphi(s^{c_2}l)$ into the kinetic equation (16) yields then:

$$\frac{3c_1 s^{3c_2-1}}{z}\varphi(z) + 3c_2 s^{3c_2-1}\varphi'(z) = -2z^2\varphi(z) + 24\int_z^{\infty}\varphi(\tilde{z})(\tilde{z}-z)\,\mathrm{d}\tilde{z}. \tag{27}$$

The scaling Ansatz implies that the lhs of equation (27) is independent of s. Hence we find that $c_2 = 1/3$, corresponding to $c_2 = 1/\lambda = 1/[\alpha(m+1)+1]$ for $m = 1$ and $\alpha = 1$. Now the sum of the lengths of all fragments equals the length of the initial segment: $\int_0^{\infty} l\,n(l,s)\,\mathrm{d}l = s^{c_1-2c_2}\int_0^{\infty} z\,\varphi(z)\,\mathrm{d}z = \text{const}$. Therefore c_1 is given by $c_1 = 2c_2 = 2/3$. Consequently, equation (27) results in

$$\frac{2\varphi(z)}{z} + \varphi'(z) = -2z^2\varphi(z) + 24\int_z^{\infty}\varphi(\tilde{z})(\tilde{z}-z)\,\mathrm{d}\tilde{z}. \tag{28}$$

Differentiating equation (28) with respect to z and defining a new function $\Phi(z)$ through $\Phi(z) = -\int_z^{\infty}\varphi(\tilde{z})\,\mathrm{d}\tilde{z}$ leads to the following linear third-order ordinary differential equation:

$$\Phi'''(z) = 24\Phi(z) + \Phi'(z)\left(\frac{2}{z^2} - 4z\right) - \Phi''(z)\left(\frac{2}{z} + 2z^2\right). \tag{29}$$

Because of the normalisation of ϕ, we have the boundary condition $\Phi(0) = -1$. Furthermore both $\Phi'(0) = 0$ and $\Phi(\infty) = 0$ hold, the first since $\varphi(0) = 0$ and the second by the definition of Φ. We note that in the limit $z \to 0$ the singularities on the rhs of equation (29) vanish, so that we have $\Phi'''(0) = 12\Phi(0)$.

We have found the solution of equation (29) numerically using the ordinary differential equation solver

COLNEW [35]. Here we solved equation (29) in the finite interval $[0, z_\mathrm{b}]$ and increased z_b until the results were independent of z_b. If $\Phi(z)$ is known, the average fragment length $\langle l\rangle$ and the fragment length distribution $p(\zeta)$ with $\zeta = l/\langle l\rangle$ follow as $\langle l\rangle = s^{-1/3}\int_0^\infty z\,\varphi(z)\,\mathrm{d}z$ and $p(\zeta) = \varphi(z)\int_0^\infty \tilde{z}\,\varphi(\tilde{z})\,\mathrm{d}\tilde{z}$. Clearly, $\langle l\rangle$ decays as $s^{-1/\lambda}$, as already derived in references [12,15] and in the previous section.

The procedure which has been outlined here for $\alpha = 1$ can be generalized to all integer α values. Introducing the function

$$\Phi_n(z) = \frac{(-1)^n}{\Gamma(n-1)}\int_z^\infty (\tilde{z}-z)^{n-1}\varphi(\tilde{z})\,\mathrm{d}\tilde{z} \qquad (30)$$

for $n \geq 1$ and setting $\Phi_0(z) \equiv \varphi(z)$, we obtain by inserting $n(l,s) = s^{c_1}\varphi(s^{c_2}l)$ into equation (16):

$$\begin{aligned}\varphi''(z) = {} & \varphi(z)\left[-\frac{2(\alpha+1)(2\alpha+1)z^{2\alpha-1}}{3} + \frac{2\alpha}{z^2}\right] \\ & + \varphi'(z)\left[-\frac{2(2\alpha+1)z^{2\alpha}}{3} + \frac{\alpha-3}{z}\right] \\ & + (-1)^{\alpha-1}\alpha!(2\alpha+1)2^{2\alpha+1}z^{\alpha-1}\Phi_\alpha(z). \qquad (31)\end{aligned}$$

Because of $\varphi^{(i)}(z) = \Phi_n^{(n+i)}(z)$, equation (31) is a linear ordinary differential equation for $\Phi_\alpha(z)$. The boundary conditions are $\Phi_\alpha^{(k)}(\infty) = 0$ for $0 \leq k \leq \alpha - 1$ and $\Phi_\alpha^{(\alpha-1)}(0) = -1$, as well as $\Phi_\alpha^{(\alpha)}(0) = 0$. Again, equation (31) can be solved numerically using COLNEW.

5 Comparison with simulations

In this section we compare the analytical and numerical results for $\langle l\rangle$ and $p(\zeta)$ (based on Eq. (15) and the previous discussion) with the outcome of stochastic simulations. To be able to achieve quickly the asymptotic situation in the simulations (which need on the one hand large systems in order to avoid discreteness and finite-size effects, and on the other hand many realizations due to the extreme-value character of the breakage process) we apply a hottest-bond algorithm which uses directly equation (4). This scheme turns out to be effective. At the beginning of the simulation, each spring of the coating is attributed a random strength according to equation (7). Then the stress in each segment is determined using equation (4); the overall shape of the stress distribution in each segment is assumed not to change with increasing load. Thus the "hottest" bond, *i.e.* the one with lowest strength to stress ratio, is the next one to break. Because of the scaling form of equation (4) with respect to ε, the failure strain is easily determined. The spring which breaks is removed from the system irreversibly and two new segments are created. In order to obtain the fragment length distribution, this procedure is iterated for 10 000 breakage events in a system of 2×10^6 springs.

Figure 2 shows the results for the mean fragment length $\langle l\rangle$ for linear stress transfer ($m = 1$) and for

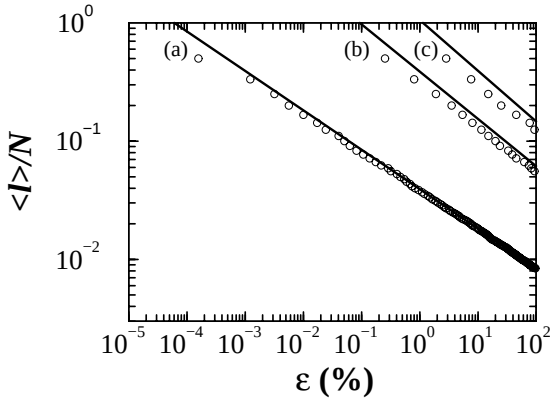

Fig. 2. The average fragment length $\langle l\rangle$ *vs.* applied strain ε in the case of linear stress transfer ($m = 1$) plotted for (a) $\alpha = 1$, (b) $\alpha = 2$ and (c) $\alpha = 3$. The circles are the results of stochastic simulations with $N = 2 \times 10^6$ and $\omega = 1$ after averaging over 10 realizations. The solid lines correspond to equation (19).

$\alpha = 1, 2, 3$ in a double-logarithmic representation. In such a representation scaling relations are straight lines. In Figure 2 the solid lines give the analytical solution, equation (19), and the circles depict the simulation data after averaging over 10 realizations. We emphasize that the strain ε in Figure 2 relates to the substrate. The strain in the coating is much smaller than ε. This assumption has been made to obtain the approximate solution of equation (3). Therefore a large strain in the substrate does not imply a large (with respect to elasticity limit) strain in the coating, and the large range of substrate strain does not violate the assumption of linear elastic coating behaviour. The simulations were performed up to a very large strain range in order to exemplify more clearly the asymptotic behaviour of the scaling relation for the average fragment length. From Figure 2 we infer the good agreement between the simulated mean fragment lengths and the analytical solution, equation (19), of the form $\langle l\rangle = c\varepsilon^{-\kappa}$; note that not only the slopes, but also the values of c are in agreement. We remark that equation (19) turns out to be valid also for nonlinear stress transfer; the scaling of $\langle l\rangle$ with ε has been already demonstrated for values of m larger than one in reference [15], and an additional investigation for $m = 3$ and $m = 5$ (which we do not report here) shows that also the prefactor of equation (19) is supported by the simulations.

Figure 3 shows the fragment length distribution for the same parameters as in Figure 2. The circles are the simulation data. The solid line displays the analytical solution equation (21) and the dashed line is obtained from the numerical solution of equation (31). The distribution $p(\zeta)$, with $\zeta = l/\langle l\rangle$, becomes more narrow for increasing α, since larger α values imply less scatter in the coating's strength. Consequently, for large α the fragments tend to break in their middle, which implies a narrow fragment length distribution. Comparing the simulations with the analytical result equation (21) shows that the agreement is reasonable, but the deviations increase with increasing α.

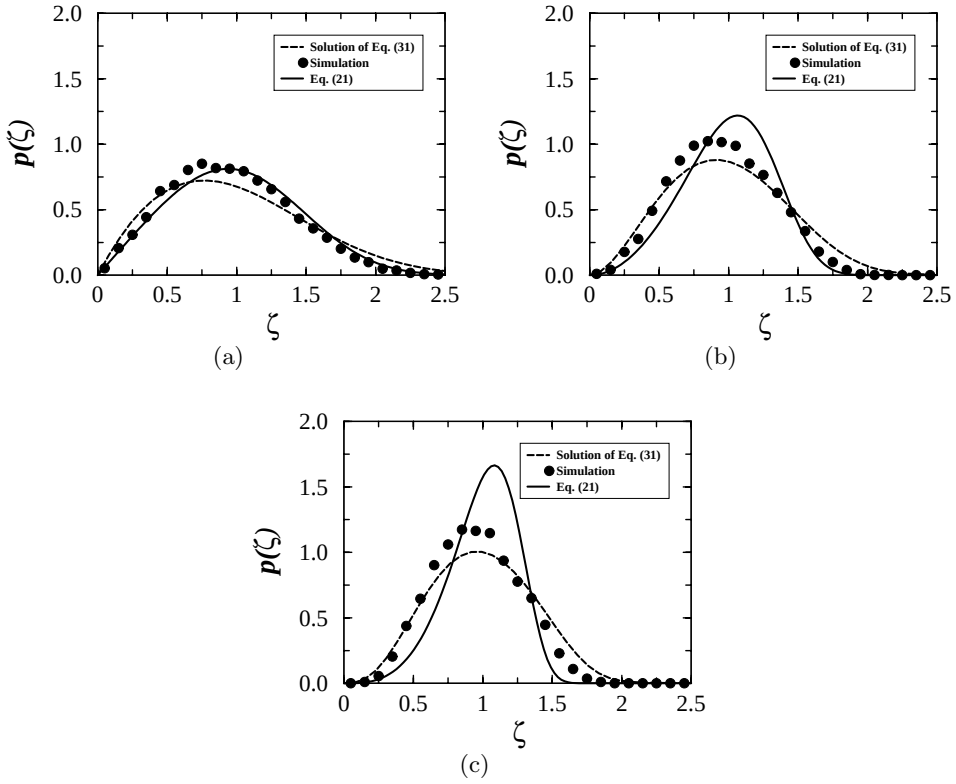

Fig. 3. The fragment length distribution $p(\zeta)$ with $\zeta = l/\langle l \rangle$ for $m = 1$ and for (a) $\alpha = 1$, (b) $\alpha = 2$, (c) $\alpha = 3$. The circles are the results of simulations with $N = 2 \times 10^6$ and $\omega = 1$. The dashed lines display $p(\zeta)$ derived from the numerical solution of equation (31), and the solid lines correspond to equation (21).

This trend can be understood in terms of the approximation $1 - |1 - 2l/x|^2 \approx 4l/x$ involved in going from equation (16) to equation (17); this approximation is quite rough for $x \approx 2l$ and its usefulness hence decreases when (as is the case for larger α) more and more segments break close to their middle. In Figure 3 we also display the results of the numerical integration of equation (31) used to obtain $p(\zeta)$ (dashed lines in Figs. 3a-c). The difference between the numerical approach based on equation (31) and the stochastic simulations is possibly due to the fact that the rate equation equation (16) does not consider the non-monotonic loading history of each element: In the simulations the weakest bonds disappear first from the system. This aspect is not taken into account in the fragmentation equation, based on a history-independent probability of failure.

Let us now discuss the case $m \neq 1$, *i.e.* nonlinear stress transfer. First we analyze the case $m \ll 1$, that of nearly perfect plasticity. We take $m = 0.05$ and $\alpha = 1$, for which we plot in Figure 4 the fragment length distribution; in the Figure the circles give the simulation results and the solid line the analytical solution equation (21). Now for $m = 0.05$ the approximation $1 - |1 - 2l/x|^{m+1} \approx 2(m+1)l/x$ is quite adequate for $x \gg 2l$. Hence one expects a satisfactory agreement between simulations and equation (21). Indeed in Figure 4, the difference between the simulation data and the analytical solution is small.

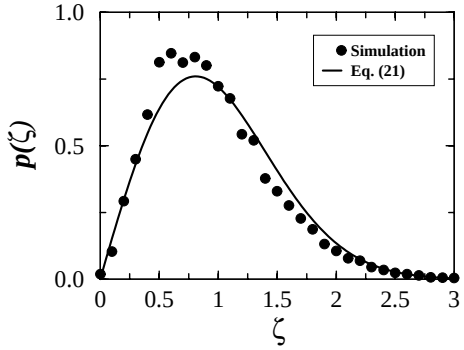

Fig. 4. The function $p(\zeta)$ with $\zeta = l/\langle l \rangle$ for $m = 0.05$ and $\alpha = 1$. The agreement between the theoretical curve equation (21) (solid line) and the results of the simulations (circles) is satisfactory, see text for details.

Continuing the study of nonlinear stress transfer we turn now to cases where $m > 1$ holds. We plot in Figure 5 the fragment length distribution $p(\zeta)$, as obtained through simulations for $\alpha = 1$ and $m = 3, 7$ and 31. Comparing the fragment length distributions for different m it turns out that with increasing m the maxima of the distribution decrease and that the distributions "flatten". This can be visualized with help of the analytical approximate solution of the kinetic equation for m very large, namely

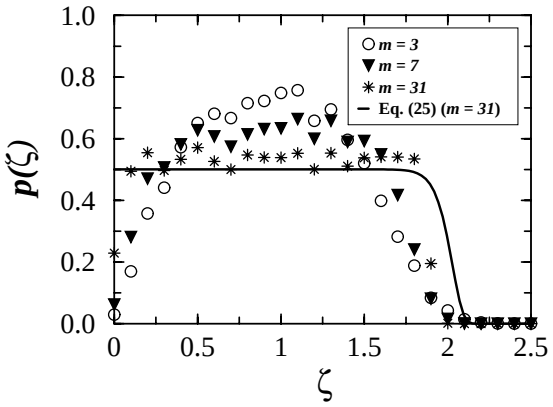

Fig. 5. The fragment length distribution $p(\zeta)$ with $\zeta = l/\langle l \rangle$ for $m = 3, 7$ and 31. The parameters are $\alpha = 1, \omega = 1$ and $N = 2 \times 10^6$. The solid line represents the analytical solution equation (25) for $m = 31$.

equation (25). In Figure 5 equation (25) is also plotted for $m = 31$ as a full line. It turns out that equation (25), which shows an almost perfect plateau behaviour, reproduces the simulation findings for $m = 31$ very well.

6 Conclusions

In this study we have modelled fragmentation in brittle coatings under uniaxial stress. We have utilized both analytical and also numerical methods. In the analysis we started from a rate equation for the fragmentation using a two-parameter Weibull distribution for the local fracture strength. We have investigated both linear and also nonlinear shear stresses between coating and substrate, and focused especially on the scaling situation in advanced stages of fragmentation. We derived an approximate solution for the fragmentation equation, which leads to *analytical* expressions for the fragment length distribution and its mean value. These findings were then confronted with numerical solutions of the fragmentation equation, as well as to simulations of the process. The dependence of the analytically determined mean fragment length on the applied strain and the fragment length distribution are found to agree with the simulations, and we discussed the achieved accuracy as a function of the parameters involved. The numerical solutions of the rate equation are also in agreement with the simulation data.

J. Andersons gratefully acknowledges the support by the DAAD which provided the opportunity for a research stay at Freiburg University. The authors are indebted to the DFG, to the GIF (project I 0423-061.14), to the PROCOPE-DAAD program and to the Fonds der Chemischen Industrie for support.

References

1. M. Marder, J. Fineberg, Physics Today, September, 24 (1996).
2. B.K. Chakrabarti, L.G. Benguigui, *Statistical Physics of Fracture and Breakdown in Disordered Systems* (Clarendon Press, Oxford, 1997).
3. Y. Leterrier, L. Boogh, J. Andersons, J.-A.E. Månson, J. Polym. Sci. B **35**, 1449 (1997).
4. U.A. Handge, I.M. Sokolov, A. Blumen, E. Kolb, E. Clément, J. Macromol. Sci. B Phys. **38**, 971 (1999).
5. U.A. Handge, Y. Leterrier, J.-A.E. Månson, I.M. Sokolov, A. Blumen, Europhys. Lett. **48**, 280 (1999).
6. C. Allain, L. Limat, Phys. Rev. Lett. **74**, 2981 (1995).
7. A. Groisman, E. Kaplan, Europhys. Lett. **25**, 415 (1994).
8. G. Müller, Physikalische Blätter **55**, No. 10, 35 (1999).
9. S. Kitsunezaki, Phys. Rev. E **60**, 6449 (1999).
10. P. Meakin, Science **252**, 226 (1991).
11. H. Colina, L. de Arcangelis, S. Roux, Phys. Rev. B **48**, 3666 (1993).
12. O. Morgenstern, I.M. Sokolov, A. Blumen, Europhys. Lett. **22**, 487 (1993).
13. A. Mézin, Acta Metall. Mater. **43**, 3151 (1995).
14. A. Mézin, B. Sajid, Thin Solid Films **358**, 46 (2000).
15. U.A. Handge, I.M. Sokolov, A. Blumen, Phys. Rev. E **61**, 3216 (2000).
16. U.A. Handge, I.M. Sokolov, A. Blumen, J. Phys. Chem. B **104**, 3881 (2000).
17. I.L. Menezes-Sobrinho, J.G. Moreira, A.T. Bernardes, Eur. Phys. J. B **13**, 313 (2000).
18. O. Morgenstern, I.M. Sokolov, A. Blumen, J. Phys. A **26**, 4521 (1993).
19. T. Hornig, I.M. Sokolov, A. Blumen, Phys. Rev. E **54**, 4293 (1996).
20. J. Andersons, V. Tamuzs, Compos. Sci. Tech. **48**, 57 (1993).
21. J. Andersons, R. Joffe, R. Sandmark, Mech. Compos. Mater. **31**, 26 (1995).
22. W.A. Curtin, J. Mater. Sci. **26**, 5239 (1991).
23. W.A. Curtin, H. Scher, Phys. Rev. B **55**, 12038 (1997).
24. W.A. Curtin, M. Pamel, H. Scher, Phys. Rev. B **55**, 12051 (1997).
25. E.J. Gumbel, *Statistics of Extremes* (Columbia University Press, New York, 1958).
26. I.M. Sokolov, A. Blumen, Physica A **266**, 299 (1999).
27. P. Meakin, Thin Solid Films **151**, 165 (1987).
28. H.L. Cox, Br. J. Appl. Phys. **3**, 72 (1952).
29. R. Hill, *The Mathematical Theory of Plasticity* (Clarendon Press, Oxford, 1998).
30. W. Weibull, J. Appl. Mech. **18**, 293 (1951).
31. S. Redner, in *Disorder and Fracture*, edited by J.C. Charmet, S. Roux, E. Guyon, NATO ASI Series B: Physics, Vol. 235 (Plenum Press, New York, 1990), Chap. 3, p. 31.
32. S. Redner, in *Statistical Models for the Fracture of Disordered Media*, edited by H.J. Herrmann, S. Roux (North-Holland, Amsterdam, 1990), Chap. 10, p. 321.
33. R. Englman, J. Phys. Condens. Matter **3**, 1019 (1991).
34. M. Baudequin, G. Ryschenkow, S. Roux, Eur. Phys. J. B **12**, 157 (1999).
35. U.M. Ascher, R.M.M. Mattheij, R.D. Russell, *Numerical Solution of Boundary Value Problems for Ordinary Differential Equations* (SIAM, Philadelphia, 1995).